THOMSON REUTERS ENDNOTE
[Tarkhan, 5(1): January, 2016]
ISSN: 2277-9655
(I2OR), Publication Impact Factor: 3.785

IJESRT
INTERNATIONAL JOURNAL OF ENGINEERING SCIENCES & RESEARCH TECHNOLOGY

SHEAR CAPACITY OF PRE-STRESSED HOLLOW CORE SLABS UNDER CONCENTRATED LOAD

Ali N. Deeb[1], Mohamed A. Tarkhan[*], and Esam M. El-Tehewy[2]
[1] PhD Student, Civil Engineering Department, Syrian Armed Forces, Syria.
[*] Correspondence author, Associate Professor at Civil Engineering Department, Faculty of Engineering-Elmattaria, Helwan University, Cairo, Egypt.
E-mail : mo_tarkhan@yahoo.com
[2] Associate Professor at Military Technical College, Cairo, Egypt.

ABSTRACT
Precast pre-stressed hollow core (PHC) slabs are considered one of the best structural systems capable of covering large spans with minimum overall thickness and weight, and its ease of manufacturing and installation. The shear resistance of PHC slabs has not been well discussed in the different current codes. The codes have a general shear design approach. However, the shear behavior of PHC slabs is different from that of ordinary concrete elements with shear reinforcement. On the other hand, the design models of PHC slabs in current codes does not take into consideration the significant effect of concentrated load at transfer zone as well as no method to classify the expected mode of failure. In this research, a new proposed relationship is developed to calculate shear capacity of PHC slabs. Also, the significant effect of variation of concentrated load width with respect the slab width will be studied. The proposed relation will be verified for different slab thickness, level of pre-stressing, concrete strength, and for solid net area of PHC slabs. Instead of performing a costly experimental study to find out whether the effect of different factors on the prediction of shear behavior of PHC slabs, a numerical model (ANSIS 11) can be used after calibrating its accuracy with experimental data of two pre-stressed hollow core slabs. The comparisons are made for load-deflection curves, failure loads and crack patterns. The accuracy of the finite element models which is assessed by comparison with the experimental results was in good agreement.

KEYWORDS: Pre-stressed hollow core slabs; Shear failure; Finite-element analysis.

INTRODUCTION
Precast, pre-stressed hollow core slabs (PHC slabs) are among the most commonly used load bearing concrete elements in the world. They are widely used in floors and roofs of office, residential, commercial and industrial buildings [1]. These units were developed in the 1950s, when long-line pre-stressing techniques evolved. For more than 30 years, the type of units produced changed little. Extensive research performed in Europe in the 1980s, led to technology advances allowing the economical production of hollow core units.
In order to verify the shear capacity of PHC slabs, a suitable test set-up must be designed to take into account all variables, which may contribute either negatively or positively to the shear capacity of the slabs. The selection of the type of the applied load used for a shear test can also have an effect on the member behavior [2]. A common approach for shear testing is to use a concentrated load, resulting in shear forces that are essentially constant between the load and the support reaction. Four full-scale tests on one-way floor systems of are performed in order to investigate the shear capacity behavior of local production PHC slabs and to check the obtained results of ANSYS program [3]. The finite element (FE) method is now well accepted as the most powerful general technique for the numerical solution of a variety of engineering problems. In the realm of linear analysis, the FE method is now widely used as a design tool [4]. The geometric shape of voids made in the cross-sections could have an impact on the web-shear capacity of PHC slabs, because the void shape affects the location of the maximum principal tensile stress in the slab, which is the main player in positioning the critical point [5]. The codes have a general shear design approach [6, 7, and 8]. However, the shear behavior of PHC slabs is different from that of ordinary concrete elements with shear reinforcement. On the other hand, the design models of PHC slabs in current codes does not take into consideration the significant effect of concentrated load at transfer zone as well as no method to classify the expected mode of failure.

ISSN: 2277-9655
(I2OR), Publication Impact Factor: 3.785

RESEARCH SIGNIFICANCE

This study presents the results of the parametric study conducted using the developed finite element model as presented above (ANSYS 11). The study investigates the effect of two key parameters that are expected to influence the shear capacity of PHC slabs. Those two parameters are:

- The shear span of the simply supported slabs, a.
- The ratio of the load width to slab width, b_s/b_L.

In the addition of the last two parameters, the research studies the following parameters:

- Slab Thickness
- Pre-stressing stress Level.
- Concrete strength.
- Solid net area ratio.

EXPERIMENTAL PROGRAM

Two prefabricated hollow core slabs are tested under concentrated load. The slabs have the same cross-section and pre-stressing strand, with dimensions of 3500 mm length, 1200 m width and 150 mm height, respectively. Each slab has twelve elliptical-shaped openings, and one oblong-shaped in the mid of slabs width. It is reinforced by eight pre-stressing seven-wire strands by along its bottom surface, as shown in Figure 1. Tables 1 and 2 summarize the details of the slab properties and pre-stressing strands, respectively.
The PHC slabs are supported on the top flanges of two I-beams and loaded with a concentrated load *P*, as shown in Figure 2. Figure 3 shows the details of the tested hollow core slabs, the load acts on an I-beam with a length equal to the width of tested slab at the distance (*a*) of 2*h* (300 mm) for tested slab SA and 3*h* (450 mm) for tested slab SB, where (*a*) is the distance from the centre line of the applied load to the middle of the bearing surface, and (*h*) is the slab thickness, respectively. The load was applied in increments of 10 kN.


Figure 1: Details for tested PHC slabs and pre-stressing strands


Figure 2: Test set-up and instrumentation for the tested PHC slabs

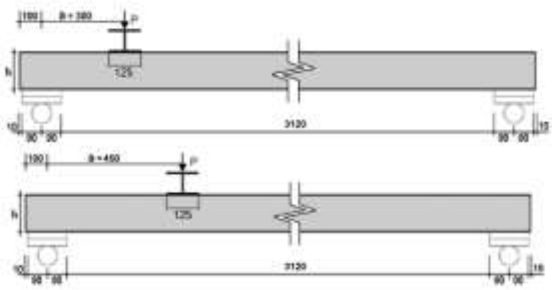
Figure 3: Loading of tested hollow-core slabs SA and SB

Table 1: Properties of hollow-core slab

Slabs	Slab length (mm)	Nominal slab height, *h* (mm)	Nominal slab depth, *d* (mm)	Shear span, *a* (mm)	*a* / *h* ratio	Net area of slab section (mm^2)	Compressive strength (f_{cu}) (N/mm^2)	Pre-stressing force (kN)
SA	3500	150	123	300	2	123440	43.57	518
SB	3500	150	123	450	3	123440	43.57	518

Table 2: Properties of pre-stressing seven-wire strands

Strands	Cross section (mm^2)	Nominal diameter (mm)	Mass (g/m)	Breakingload (kN)	Ultimate strength (N/mm^2)	Yield strength (N/mm^2)	Modulus of elasticity (N/mm^2)
7-wire	54.84	9.53	432	102.3	1860	1679	197500

ISSN: 2277-9655
(I2OR), Publication Impact Factor: 3.785

FINITE ELEMENT MODELING

To simulate the behavior of the tested PHC slabs under the effect of a concentrated load, the finite element software ANSYS 11 is used. Two types of elements SOLID65 and LINK8 are selected to model concrete and pre-stressed steel tendons, respectively. The material properties defined for each type of element in the finite element model are based on the standard test.

Model Verification

Load-Deflection Curves

The deflections of the tested PHC slabs at each applied load increment were taken from the output results to construct the load-deflection curves and the crack propagation was observed for each model. The failure point is determined in the analytical model at the load value, where the computer program indicates suddenly large deflection. The maximum nominal load of a specimen was used as an index in the comparison of the two sets of results. For all models, the load-deflection curves of concrete were recorded at middle width of slabs on the bottom surface at two locations: first directly under vertical load, second at point A (were the maximum deflection occurred) as shown in Figure 4.

A comparison between the experimental and numerical load-deflection curves for the tested PHC slabs are shown in Figures 5 to 8, respectively. It is clear that the failure mode of the analytical model is similar to that in the experimental model, and behaves in the same manner. The curves show good agreement between the finite element analysis and the experimental results throughout the entire range of behavior and failure mode.

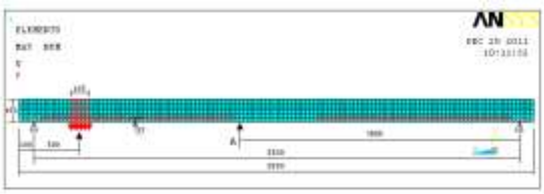

Figure 4: Location of the recorded deflection (Under vertical load and at point A)

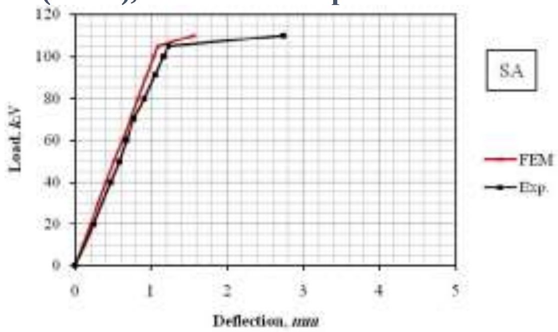

Figure 5: Load-deflection curves for tested PHC slab SA (At point under vertical load) [3]

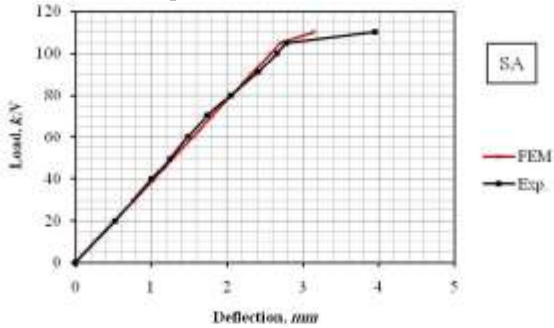

Figure 6: Load-deflection curves for tested PHC slab SA (At point A of max. deflections) [3]

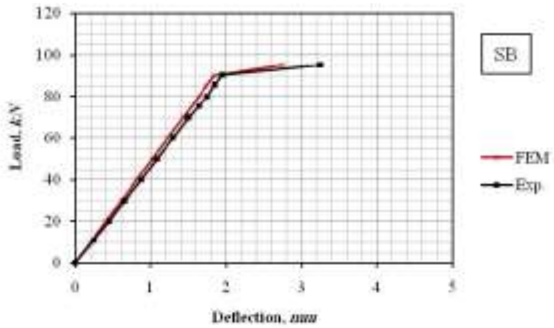

Figure 7: Load-deflection curves for tested PHC slab SB (At point under vertical load) [3]

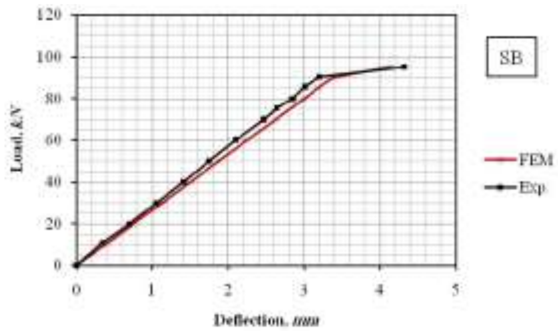

Figure 8: Load-deflection curves for tested PHC slab SB (At point A of max. deflections) [3]

Crack Pattern and Modes of Failure

After the initiation of shear cracks, the stiffness of the tested PHC slabs was reduced and the load-deflection behavior ended when the failure occurs. In the actual slabs, the failure is abrupt and noisy, like a small explosion. When the first crack appears, the failure takes places immediately. Figure 9 shows the evolution of crack patterns developing for each slab at the failure. The failure modes of the finite element models show a good agreement with observations and data from the experimental full-scale slabs. In the actual slabs the failure mode appearing as web-shear failure near the support for tested slab SA and flexural-shear failure under the vertical load for the tested slab SB. The web-shear failure is accompanied with anchorage failure in the eight strands in slab SA, as shown in Figure 10, but anchorage failure is occurred at the two middle strands in slab SB, as shown in Figure 11. In the finite element models, the failure mode appears as shear failure under vertical load for both slabs.

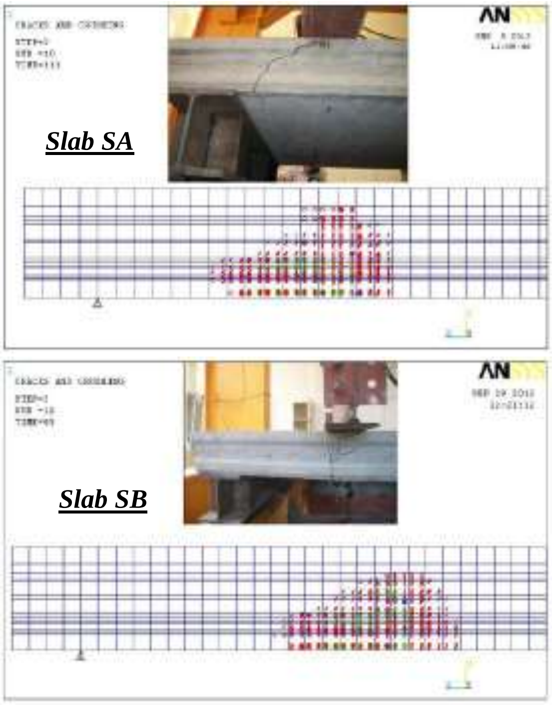

Figure 9: Side crack pattern and failure modes for tested PHC slab SA and SB [3]

Figure 10: Anchorage failure of the eight strands in SA

Figure 11: Anchorage failure of the two middle strands in SA

From the above verification, it can be conclude that the developed finite element model showed a good agreement between the experimental load deflection relationship, failure load, and cracks results. This indicates that the developed numerical models in the current study accurately predicted. Therefore, the developed finite element model for this research is given more confidence in the use of ANSYS program and suitable for use in further parametric studies.

THEORITICAL ANALYSES

This section presents the results of the parametric study conducted using the developed finite element model as presented above. The study investigates the effect of research parameters mentioned above. The used model in this parametric study had the same geometric details, concrete and strand material properties of the model that is presented to simulate slab. The studied variables are altered with a wide range to practically cover the effect of the parameter on the shear behavior of the PHC slabs. Outputs from model solutions are compared in terms of the load at first cracks. The following sections outline these results and the discussion for the investigated parameters. The following sections will discuss the last parameters.

ISSN: 2277-9655
(I2OR), Publication Impact Factor: 3.785

Effect of Shear Span

There is a lack of research data in the literature about the critical shear span for the minimum diagonal shear resistance of PHC slabs. Cheng and Wang [9] presented data about the effect of shear span in 200 mm PHC slabs with circular voids. There was no data found regarding effect of shear span on other slabs with non-circular voids. Therefore, this study will investigate the effect of shear span on the shear capacity of slabs with non-circular voids and the developed FEM is used for this purpose. This investigation is performed by changing the location of the applied vertical line load on the model. The shear span is related to the average depth of slabs (h = 150 mm) by the shear span-to-depth ratio (a / h). Different a / h ratios, ranged from 2.0 to 6.0, are investigated. The load-deflection results from this parametric study are presented for slabs plotted at the mid-point of the slab. The obtained load deflection graphs for the slab are shown in Figure 12. As expected, the deflection increased with increasing the shear span due to of increasing the bending moment at load position.

Figure 13 presents ultimate failure loads versus a / h ratio. According to the results of this conducted parametric study, it can be observed that the most critical shear capacity for the simulated 150 mm PHC slab with non-circular voids has decreased by increasing the shear span. Also, it can be observed that the shear capacity decreased rapidly and clear with increasing the shear span until the ratio is about 4. After that, the shear capacity began decreasing slightly. The increase in the shear capacity, in case of a / h = 2, is about 30% more than in case of a / h = 4. Moreover, the shear capacity was 3.7% lesser than in case of a / h = 5, which appeared to fail due to flexural and shear mode.

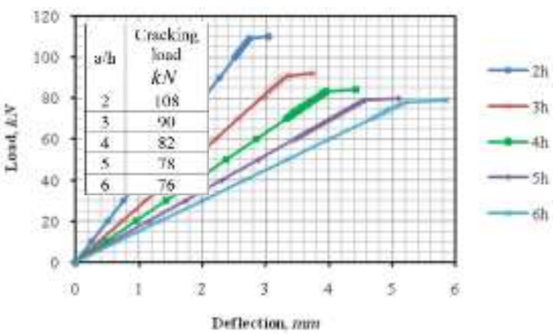

Figure 12: Load-deflection curves for different shear span of PHC slab

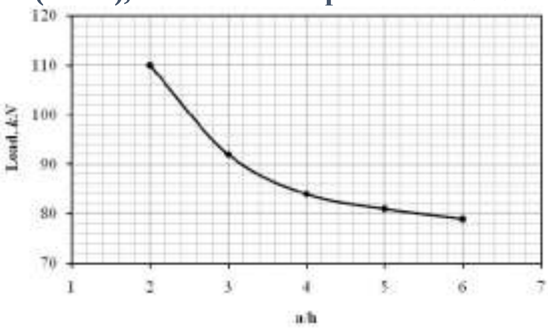

Figure 13: Ultimate failure loads versus a / h ratio

Effect of Load Width

To study the effect of the load width on the shear capacity of the PHC slab, thirty six case of study were presented. The level of load width was presented through nine cases for every shear span. The load width (b_L), Fig 14, ranged from 1200 to 416 mm, as shown in Table 3, while the shear span (a) is taken as 2h, 3h, 4h and 5h, respectively. The ultimate strength of full width of applied load is taken as the control case for each the other shear span to comparing the other results. These different levels of load width are simulated by changing the width of the applied load, which is symmetrically with the longitudinal axis of the tested slabs. Table 3 summarizes the cracking and failure load obtained from the theoretical study. The results shown in the Table 3 indicates the significant effect of the applied load width, and show that capacity decreases with decreasing the load width. In addition, it can be observed from Figure 15 that the shape of load-deflection curve is almost the same in all cases in elastic stage. On the other hand, it can be seen that whilst the applied load width is increasing, the brittle failure is occurred in all studied cases. This width of the load at which the failure to be brittle is changed by changing the shear span value. For example, increasing the shear span from 3h to 4h, the width ratio at which the mode of failure changed to brittle failure is 43% and 50% respectively.

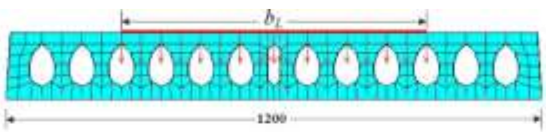

Figure 14: Variation of load width

ISSN: 2277-9655
(I2OR), Publication Impact Factor: 3.785

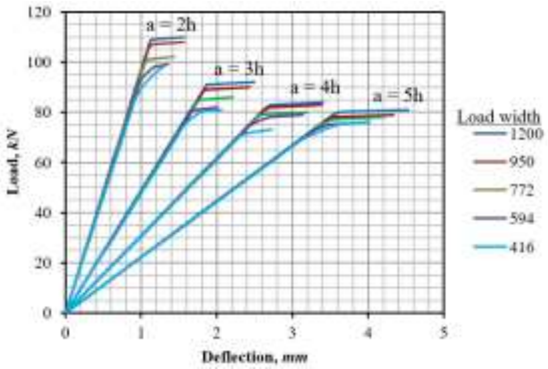

Figure 15: Load-deflection curves for different load width versus a / h ratio of slab

Table 3: Theoretical results for different load width versus the a/h ratio of slab

Load Width		Slab (*L=3500 mm*)							
b_L	(b_L/1200) %	P at $a = 2h$		P at $a = 3h$		P at $a = 4h$		P at $a = 5h$	
		P_{Cracks}	$P_{Failure}$	P_{Cracks}	$P_{Failure}$	P_{Cracks}	$P_{Failure}$	P_{Cracks}	$P_{Failure}$
1200	100	108	110	90	92	82	84	78	81
1039	86.58	108	110	90	92	82	84	78	80
950	79.16	105	108	88	90	81	83	77	79
861	71.75	102	105	86	88	79	82	76	78
772	64.33	99	102	84	86	78	80	75	78
683	56.91	95	98	82	84	76	79	73	75~77
594	49.5	92	94	80	82	74	76~79	72	74~76
505	42.08	88	92	77	79~81	72	74~79	70	72~76
416	34.66	84	87	75	76~81	70	72~73	69	70~75

Table 4: Theoretical results of ratio bLi/bs and Pi/Pmax

Load width		P_{crack}	P_i/P_{max}	P_{crack}	P_i/P_{max}	P_{crack}	P_i/P_{max}	P_{crack}	P_i/P_{max}
b_{Li}	b_{Li}/b_S	$a/h = 2$	$P_i/108$	$a/h = 3$	$P_i/90$	$a/h = 4$	$P_i/82$	$a/h = 5$	$P_i/78$
1200	1	108	1	90	1	82	1	78	1
1039	0.8658	108	1	90	1	82	1	78	1
950	0.7917	105	0.9722	88	0.9778	81	0.9878	77	0.9872
861	0.7175	102	0.9444	86	0.9556	79	0.9634	76	0.9744
772	0.6433	99	0.9167	84	0.9333	78	0.9512	75	0.9615
683	0.5692	95	0.8796	82	0.9111	76	0.9268	73	0.9359
594	0.495	92	0.8519	80	0.8889	74	0.9024	72	0.9231
505	0.4208	88	0.8148	77	0.8556	72	0.8781	70	0.8974
416	0.3467	84	0.7778	75	0.8333	70	0.8537	69	0.8846

Relation between Shear Span and Load Width

Based on the results in Table 3, there is some relation between them. Since the difference between the first cracking load and failure load is very small, we consider the first cracking load is the failure load. Depending on the values in Table 3 and considering the load obtained at b_s is the maximum load (P_{max}) for all cases of shear span-to-depth ratio, we can write the Table 4 and draw the curves shown in Figure 16 and their modified curves shown in Figure 17. From curves shown in Figure 17, the linear equation for studied cases of different shear span-to-depth ratios are given in Table 5 along the

ISSN: 2277-9655
(I2OR), Publication Impact Factor: 3.785

correlation coefficient R^2. From Table 5, it can be noted that all equations have a form of type:

$$y - y_o = \propto (x - x_o) \qquad (1)$$

Equation 1 can be written in other form as:

$$y = \propto (x - x_o) + y_o \qquad (2)$$

As shown in Figure 17, x_o and y_o are equal are constant in all equations and their values are 0.87 and 1 respectively. These equation s are different only by the value $\propto$, which represents the slope of each line, so, Equation 2 can be written as:

$$\frac{P_i}{P_{max}} = \propto \left(\frac{b_{Li}}{b_s} - 0.87\right) + 1 \qquad (3)$$

From which the constant $\propto$ is calculated. By fitting the solution points, as shown in Figure 18, we get the equation as:

$$\propto = 0.691\left(\frac{a}{h}\right)^{-0.66} \qquad (4)$$

Equation 4 can be approximated and rewritten as:

$$\propto = 0.7\left(\frac{a}{h}\right)^{-\frac{2}{3}} \qquad (5)$$

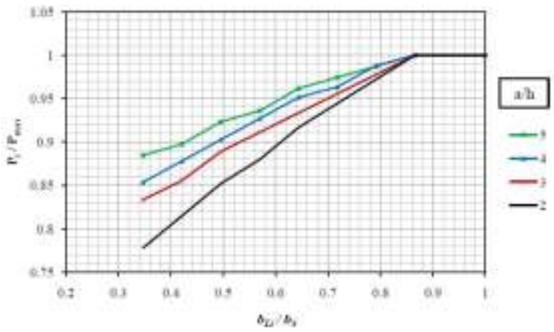

Figure 16: Relation between P_i/P_{max} and b_{Li}/b_s for different shear span a/h

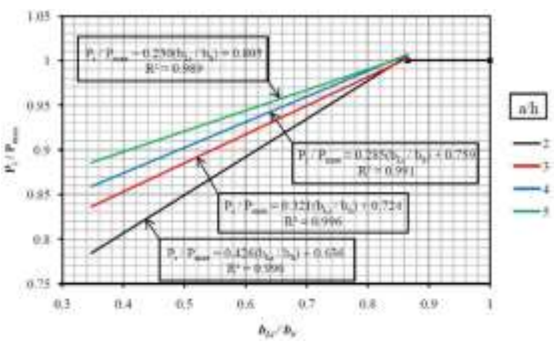

Figure 17: Linear equations for relation between P_i/P_{max} and b_{Li}/b_s for different shear span a/h.

Table 5: Linear equation for different cases of shear span-to-depth ratio

a/h	Equations	
2	$P_i/P_{max} = 0.426(b_{Li}/b_s) + 0.636$	$R^2 = 0.996$
3	$P_i/P_{max} = 0.321(b_{Li}/b_s) + 0.724$	$R^2 = 0.996$
4	$P_i/P_{max} = 0.285(b_{Li}/b_s) + 0.759$	$R^2 = 0.991$
5	$P_i/P_{max} = 0.230(b_{Li}/b_s) + 0.805$	$R^2 = 0.996$

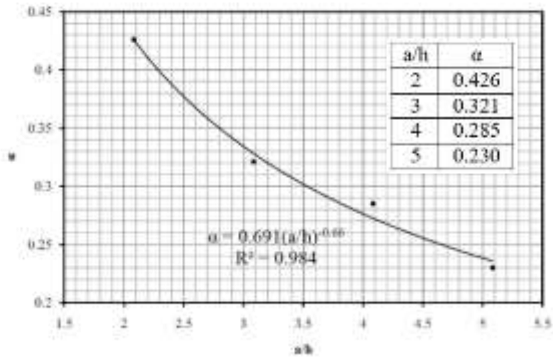

Figure 18: relation between α and a/h

Equations 3 and 5 obtained above can be used to calculate the ratio of $P_i/P_{max} = c$. This coefficient represents the effect of load width on shear capacity at different cases of shear spans. Coefficient c can be used in different shear resistance equations of ACI [6], EC-2 [7], and ECP [8] codes. So, the final equation form of Equations 3 and 5 can be expressed as:

$$\frac{P_i}{P_{max}} = c = \frac{0.7}{\left(\frac{a}{h}\right)^{\frac{2}{3}}}\left(\frac{b_{Li}}{b_s} - 0.87\right) + 1 \leq 1 \qquad (6)$$

To enable codes' equations, calculating shear capacity considering the effect of different load widths and different shear spans by multiplying the shearing force (P) with the coefficient c as follows:

$$P` = cP \qquad (7)$$

For Example: In the Egyptian Code (ECP-203) [8], the shear resistance equation of q_{cu} becomes $q`_{cu} = q_{cu}$.

Experimental Verification

To verify the equation results, two PHC slab of height 150 mm and 1200 mm width were experimentally tested. The results from tests are compared with numerical results as shown in Table 6. There is a good agreement between the two results, where the ratio is around 1.

Table 6: Ratio of factor c between experimental and equation results

Load	Test	Equation	Ratio

Width		Results			Results			
b_L (mm)	a/h	P_{max}	P_i	c_{test}	α	b_L/b_s	c_{eq}	c_{test}/c_{eq}
700	2	110	95	0.86	0.44	0.58	0.87	0.989
300	3	95	73.5	0.77	0.33	0.25	0.79	0.978

Effect of Slab Thickness

By analyzing two PHC slab of 200 mm and 300 mm height and have the same load width, shear span, concrete strength, and pre-stressing level stress, it is found that good agreement of the c ratios between FE and equation results. Therefore, the coefficient c is valid for the different slab thickness.

Effect of Pre-stressing Stress Level

By analyzing two PHC slab of 300 mm height and have the same load width, shear span, and concrete strength but varied pre-stressing level stress, it is found that good agreement of the c ratios between FE and equation results. Therefore, the coefficient c is valid for the different Pre-stressing stress level.

Effect of Concrete Strength

By analyzing two PHC slab of 150 mm height and have the same load width, shear span, and pre-stressing level stress but varied in concrete strength, it is found that good agreement of the c ratios between FE and equation results. Therefore, the coefficient c is valid for the different concrete strength.

Effect of Solid Net Area Ratio

By analyzing three PHC slab of solid net area of 0.695, 0.64, and 0.61 and the same load width, shear span, pre-stressing level stress, and concrete strength, it is found that good agreement of the c ratios between FE and equation results. Therefore, the coefficient c is valid for the different cases of solid net area ratio.

CONCLUSIONS

Based on the obtained results and discussion, the following main conclusions are extracted:

1) The numerical solution was adopted to evaluate the ultimate shear capacity of pre-stressed hollow core slabs reinforced with eight pre-stressing strands, and compared with experimental full-scale test.
2) The developed finite element model in this research can accurately simulate the shear behavior of this type (elliptical shape) of the pre-stressed concrete hollow core slab.
3) The present finite element model can be used in future studies to develop design rules for pre-stressing hollow core slab members.
4) The shear capacity of the slab decreased significantly and clear with increasing the shear span, this decreasing was 30% with increasing the shear span from 2h to 4h. After this value, the shear capacity began decreasing more slightly.
5) Increasing of the load width is lead to increase the shear capacity of the slab, but the failure go to brittle failure.
6) A coefficient c obtained through a parametric study can control the relationship between both parameters, shear span and load width, and the shear capacity of PHC slabs when different values of the mentioned parameters are considered as given in next equation.

$$\frac{P_i}{P_{max}} = c = \frac{0.7}{(\frac{a}{h})^{\frac{2}{3}}}\left(\frac{b_{Li}}{b_s} - 0.87\right) + 1 \leq 1$$

7) The coefficient c calculated by the last equation is valid for different values of parameters: slab thickness, pre-stressing stress level, concrete strength, and solid net area ratio.

REFERENCES

[1] Palmer, K. D. and Schultz, A. E. (2010). “Factors affecting web-shear capacity of deep hollow core units”. PCI Journal, 55(2):123-146.

[2] Pajari, M. (2009). “Web shears failure in pre-stressed hollow core slab”. Rakenteiden Mekanika (Journal of Structural Mechanics), 42(4): 207-217.

[3] Deeb, A. N., Tarkhan, M. A. and El-Tehewy, E. M. (2015). “Finite element modeling of pre-stressed hollow core slabs”. Current Science International, 4(4): 596-603.

[4] Yang, L. (1994). “Design of pre-stressed hollow core slabs with reference to web shear failure”. ASCE Journal of Structural Engineering, 120(9): 2675-2696.

[5] Pajari, M. (2005). “Resistance of pre-stressed hollow core slabs against web shear failure”. Espoo. Research notes 2292, VTT Technical Research Centre of Finland.

[6] American Concrete Institute ACI, (2005). “Building code requirement for structural concrete”. ACI 318-05, Michigan, USA.

[7] Europe Code 2 (EN1992-1-1). (2004). “Design of concrete structures”. Part 1: General rules and rules for buildings.

[8] Egyptian Code Committee (ECP 203-2007). (2007). “Egyptian code of practice for design and construction of reinforced concrete

structures”. Building Research Centre, Cairo, Egypt.

[9] Cheng, S. and Wang, X. (2010). “Impact of interaction between adjacent webs on the shear strength of pre-stressed concrete hollow-core units”. PCI Journal, 55(3): 46-63.

[10] Hawkins, N. M. and S. K. Ghosh, S. K. (2006). “Shear strength of hollow-core slabs”. PCI Journal, pp. 110–114.

AUTHOR BIBLIOGRAPHY

	Ali N. Deeb PhD Student, Civil Engineering Department, Syrian Armed Forces, Syria
	**Mohamed A. Tarkhan** Associate Professor at Civil Engineering Department, Faculty of Engineering-Elmattaria, Helwan University, Cairo, Egypt.
	Esam M. El-Tehewy Associate Professor at Military Technical College, Cairo, Egypt.